Modeling of Real-Shaped LTCC Stripline Structure having Sharpened Edges and Embedded Pores

Jae Hyuk Jang, Norimasa Ishitobi, and Chul Ho Kim

R&D Center, Samsung Electromechanics, Suwon, Kyunggi 442-743, Korea

Abstract — **A real-shaped LTCC stripline model including sharpened edges and embedded pores was proposed and simulated using the high frequency simulator software, HFSS. These structural defects occur when LTCC process is used in real fields. The pores made the characteristic impedance of the stripline increase, and α and β decrease in the range higher than 6 % of corresponding initial values. 6 % of β could have an important meaning for circuit designers. Sharpened edge made the characteristic impedance and α increase, while did not affect β.**

I. INTRODUCTION

Low temperature cofired ceramics (LTCC) technology offers a promising solution for RF wireless applications. This technology enables the low-cost integration of passive components into the LTCC platform [1]. One of the most important processes in manufacturing multilayer LTCC packages involves cofiring of metals and ceramics. Mismatched densification kinetics between the metal and the ceramic could generate undesirable defects, including delamination, cracks, pores, and camber in the final product [2]. Therefore, the processes that result in the above-mentioned defects must be completely understood before the processing parameters and material compositions that will minimize the possibility of forming cofiring defects are optimized. The final LTCC package, however, should have undesirable shape of edged-transmission line inevitably and could have some pores on the boundary between metal and ceramic even after very careful controls. These defects are ignored frequently by circuit designers. The objective of the work reported here is to provide predictive functions that anticipate the nonnegligible variations due to the microstructural defects applied in the real LTCC processes. The ability to quantify and predict the performance of the real LTCC package is an important requirement for future circuit design.

II. MODELS

Figure 1 shows the real microstructures of the LTCC stripline when the processing parameter and the material composition, especially the composition of organics such as binder and plasticizer, were controlled well (Fig. 1(a)) and not optimized (Fig. 1(b)). The edge of the stripline was sharpened during the lamination process of the layers. This sharpened edge is unavoidable under the LTCC process. The pores were produced during the firing process when the vaporized organics could not escape to outside. This vapor pressure combined with the stress coming from the different densification of materials might produce a crack or delamination on the boundaries between metal and ceramic [3].

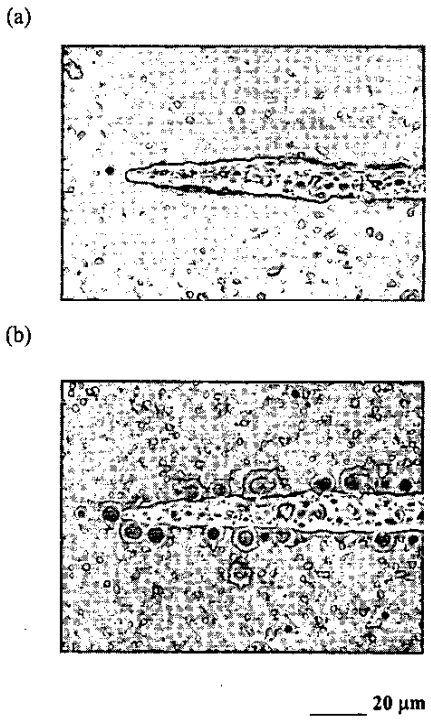

Fig. 1. (a) Microstructure of LTCC stripline when the preparation conditions were controlled well and (b) not optimized.

0-7803-7239-5/02/$10.00 © 2002 IEEE

Figure 2 gives the models of the modified striplines. The reference shape of a quarter-view stripline is shown in Fig. 2(a). The width *w*, ground-plate spacing *b*, and the thickness *t* of the stripline are 0.950 mm, 1 mm, and 0.018 mm, respectively. The dimensions of the model were decided considering the real LTCC test packages that we prepared. Figure 2(b) shows the configuration of pore arrays. The 10 μm-size pore was chosen and the gap between pores was varied from 0 μm to 40 μm. Figure 2(c) shows the different sharpness of the conductor edges. Sharpness increases as the number of model increases. Edge.1 and Edge.2 have the *e/t* (edged length/stripline thickness) ratio smaller than unity, while Edge.3 and Edge.4 have the *e/t* ratio larger than unity. Total cross-sectional area of the conductor should be same, so the stripline width *w* increases as an increase of sharpness. All models were simulated using 2 dimensional finite element method in ANSOFT HFSS software [4]. It was assumed that the models are TEM transmission lines at 2 GHz. The model including pores shown in Fig. 2(b) could not be simulated at once when 2 dimensional method was used. The results of the pore-model were obtained from combining two independent simulations, e.g. one model including pores and the other Ref.-model (without pore) in Fig. 2(c), with the appropriate mixing ratio. $\varepsilon_r = 7$ and $\tan\delta = 0$ were used for a dielectric material. Silver having the conductivity of 6.1×10^7 S/m was assigned to conductor material. Air was assigned to pore.

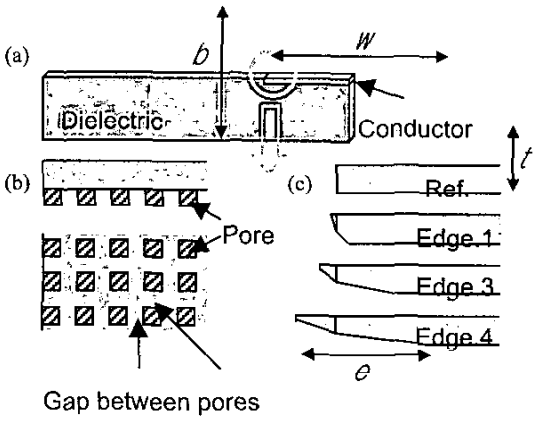

Fig. 2. (a) Reference model of the stripline, (b) Model including embedded pores, (c) Model having sharpened edges.

Figure 3 gives a mesh configuration of the stripline model. To obtain a good initial mesh condition, the increased number of rectangular sub-blocks was added in the edge-region where the field concentrated. Then, the adaptively-refined mesh function in HFSS was used. The size of the additional sub-block decreased with the factors of 0.4 or 0.5.

The relative error range of characteristic impedance was plotted as a function of total mesh number for the different sub-block conditions in Fig. 4. In the name of the sub-block condition for an example of D12L5, D12 means the dielectric consisting of 12 sub-blocks and L5 means the conductor consisting of 5 sub-blocks. D1L1 shows higher relative error values compared to the other models. The error values of D1L1 fluctuate as an increase of total mesh number. D4L1 shows the low level of error values but has the fluctuated error values. D8L1, D12L1, D12L3, and D12L5 show the decreasing error values without fluctuation as total mesh number increases. D12L5 was chosen as a reference model for the further simulations of the models including embedded pores and sharpened edges.

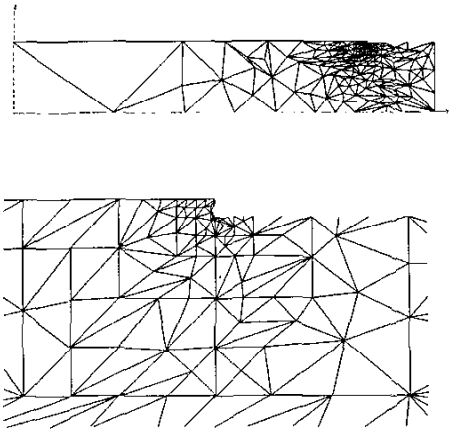

Fig. 3. Mesh configuration of the model. Rectangular squares are sub-blocks.

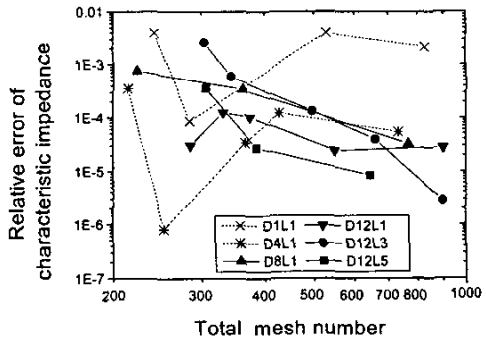

Fig. 4. The error of discretion as a function of total mesh number.

III. RESULTS AND DISCUSSION

The simulation results of the various gap width from 0 μm to 40 μm are shown in Fig. 5. The characteristic impedance was plotted as a function of gap width between the adjacent pores. As the gap width decreased (pores increased), the characteristic impedance increased slowly from no-pore to 10 μm and became to increase abruptly closer than 10 μm. The difference of the characteristic impedance between the reference stripline having no pore and the stripline having fully-linked pores like a crack or delamination was 6.24 %. Figure 6 shows the plot of attenuation constant α and phase constant β versus gap width between pores. With decreasing the gap width (with increasing pores), α decreased slowly in the region larger than 10 μm and became to decrease abruptly in the region smaller than 10 μm. α means conductive loss because tanδ of dielectric is zero in this simulation. It is assumed that the pores made conductive loss decrease according to the rate of the area occupied by the pores to the total area of the pores and the gap (Refer to Fig 2(b) bottom-view drawing). β decreased with decreasing the gap width (with increasing pores) due to the same reason. The maximum differences of the α and β were 6.7 %, 6.34 %, respectively. Shift of 6.34 % in β should have more important meaning rather than in α for circuit designers who are designing filters [5]. This β range of 6.34 % corresponds to the ε_r range of 12.28 % e.g. 6.162 minimum and 7.025 maximum.

The characteristic impedance for various sharpness of the stripline edge is shown in Fig. 7. As the sharpness increased, the characteristic impedance decreased due to the increased stripline width. The more the edge was sharpened, the wider the stripline width was, because the total cross-sectional area of the conductor should not be changed as mentioned above in Fig. 2(c). The edge-shape of the real stripline could correspond to the model of Edge.4 approximately in our LTCC processes. Figure 8 shows the plots of α and β versus sharpness of the stripline-edge. α decreased initially from the rectangular model to Edge.2, but increased from Edge.2 to Edge.4, with increasing sharpness. It could be explained using the field fringing effect. Since stripline is certainly not a parallel plate and does involve considerable fringing fields, the effect of this concentration of field distribution is significant [6]. The fields that were concentrated on the edge of the rectangular stripline were dispersed as the edge-shape changed from Ref. to Edge.2 (e/t ratio smaller than unity), while were concentrated again as the edge sharpened changed to Edge.4 (e/t ratio larger than 2). The maximum difference of α was 1.8 %. The tip of the stripline in all models having the sharpened edge was designed to have a vertically-flat region of 2 μm length to resemble the real LTCC stripline. If the sharpness of tip increased, the maximum difference of α should increase. The shape of edge did not affect β as shown in Fig. 8(b).

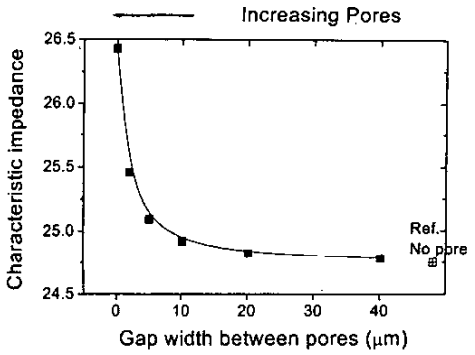

Fig. 5. Characteristic impedance as a function of gap width.

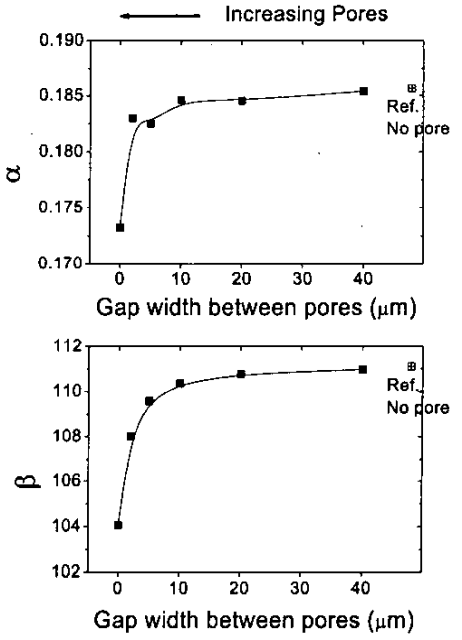

Fig. 6. Attenuation constant and phase constant as a function of gap width.

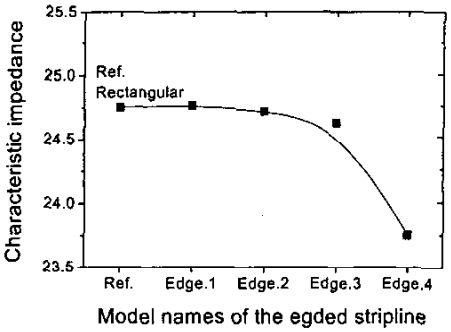

Fig. 7. Characteristic impedance as a function of sharpness of the stripline edge. Sharpness increases as an increase of model number.

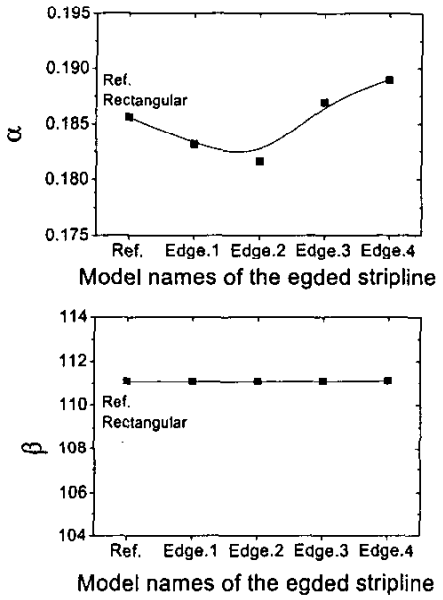

Fig. 8. Attenuation constant and phase constant as a function of sharpness of the stripline edge.

IV. CONCLUSIONS

We proposed the real LTCC stripline models including embedded pores and sharpened edges. The gap width between the pores of 10 μm-size was varied from 0 μm to 40 μm. The sharpness of the stripline-edge was varied from rectangular to sharp shape similar to the real LTCC stripline. A proper mesh condition in the models was achieved adding sub-blocks in the region where the fields concentrated and using adaptively-refined mesh function in HFSS. The pores increased, the characteristic impedance of the stripline increased, while α and β decreased more than 6 % of initial values. The 6 % of β should not be negligible by circuit designers. Sharpened edge made the characteristic impedance decrease and α increase. β was not affected by the sharpness of edge.

REFERENCES

[1] F. J. Schmuckle, A. Jentzsch, W. Heinrich, J. Butz, M. Spinnler, "LTCC as MCM substrate : Digest of strip-line structures and flip-chip interconnects," *2001 IEEE MTT-S Int. Microwave Symposium Dig.*, vol. 3, pp. 1903-1906, 2001.

[2] C.-R. Chang, J.-H. Jean, "Effects of silver-paste formation on camber development during the cofiring of a silver-based, low-temperature-cofired ceramic packagc," *J. Am. Ceram. Soc.*, vol. 81, no. 11, pp. 2805-2814, 1998.

[3] C. H. Hsueh, A. G. Evans, "Residual stress and cracking in metal/ceramic systems for microelectronic packaging," *J. Am. Ceram. Soc.*, vol. 68, no. 3, pp. 120-127, 1985.

[4] Ansoft HFSS software package, Pittsburgh, PA.

[5] G. Matthaei, L. Young, E. M. T. Jones, *Microwave Filters, Impedance-Matching Networks, and Coupling Structures*, Artech House, 1980.

[6] T. Edwards, *Foundations for Microstrip Circuit Design*, England : John Wiley & Sons, 1992.